# "Parallel" and "Antiparallel Tail-Clamps" Increase the Efficiency of Triplex Formation with Structured DNA and RNA Targets

Anna Nadal,[a] Ramon Eritja,[b] Teresa Esteve,[a] and Maria Pla*[a, c]

*Sequence-specific triple-helix structures can be formed by parallel and antiparallel DNA clamps interacting with single-stranded DNA or RNA targets. Single-stranded nucleic acid molecules are known to adopt secondary structures that might interfere with intermolecular interactions. We demonstrate the correlation between a secondary structure involving the target—a stable stem predicted by in silico folding and experimentally confirmed by thermal stability and competition analyses—and an inhibitory effect on triplex formation. We overcame structural impediments by designing a new type of clamp: "tail-clamps". A combination of gel-shift, kinetic analysis, UV thermal melting and thermodynamic techniques was used to demonstrate that tail-clamps efficiently form triple helices with a structured target sequence. The performance of parallel and antiparallel tail-clamps was compared: antiparallel tail-clamps had higher binding efficiencies than parallel tail-clamps both with structured DNA and RNA targets. In addition, the reported triplex-stabilizing property of 8-aminopurine residues was confirmed for tail-clamps. Finally, we discuss the possible use of this improved triplex technology as a new tool for applications in molecular biology.*

## Introduction

Oligonucleotides can interact in a sequence-specific manner with homopurine–homopyrimidine sequences of duplex and single-stranded DNA and RNA to form triplexes.[1] Depending on the composition and the orientation of the third strand with respect to the central homopurine Watson–Crick (WC) strand, triplexes are classified into two main categories: i) parallel and ii) antiparallel.[2]

The best-characterized parallel triplex is that formed between a double-stranded homopurine–homopyrimidine helix (duplex DNA) and a single-stranded homopyrimidine track (triplex-forming oligonucleotide). In this type of triple helix, the triplex-forming oligonucleotide binds to the major groove, parallel to the homopurine strand of the Watson–Crick double-helical DNA, through Hoogsteen hydrogen bonding and is stabilized under acidic conditions.[1,3] As an alternative approach, parallel-stranded duplexes or parallel clamps—consisting of purine residues linked to a pyrimidine chain of inverted polarity by 3′–3′ or 5′–5′ internucleotide junctions (Scheme 1)—have been designed[4–6] and demonstrated to bind single-stranded DNA and RNA targets by triplex formation.[4,5,7,8]

In the antiparallel triplexes, the third strand composed of purine bases binds antiparallel to the homopurine strand of the duplex through reverse-Hoogsteen hydrogen bonds and its binding is pH-independent.[9] The same strategy has been shown to generate stable antiparallel triplexes when purine-rich clamps are used as templates:[10–13] that is, antiparallel clamps (Scheme 1).

One of the main drawbacks of this technology is the low stability of triple helices, especially under neutral and basic pH conditions in the case of parallel triplexes. A large effort has been devoted to designing modified oligonucleotides to enhance triple helix stability.[1] One of the most successful modifications was to replace natural bases with some modified bases.[14] The introduction of an amino group at the 8-position in adenine brings with it the combined effects of a gain in one Hoogsteen purine–pyrimidine H-bond and the ability of the amino group to be integrated into the "spine of hydration" located in the minor-major groove of the triplex structure.[4] Binding of pyrimidine single strands by modified clamps containing 8-aminopurines has been described and shows high affinity for model homopyrimidine sequences, resulting in the formation of very stable triplexes.[4,15] The design of clamps capable of increasing the stability of triplex structures further would be highly desirable for the use of triple helix formation as a new tool for applications such as structural studies and DNA-based diagnostic tools, as well as for antigene and antisense therapies.[1,16–19]

A second problem for the inclusion of this technology in the molecular biology toolbox involves the placement of the

[a] *Dr. A. Nadal, T. Esteve, Dr. M. Pla*
*Departament de Genètica Molecular*
*Institut de Biologia Molecular de Barcelona (IBMB)*
*Consejo Superior de Investigaciones Científicas (CSIC)*
*Jordi Girona 18–26, 08034 Barcelona (Spain)*
*Fax: +34 93-204-5904*
*E-mail: maria.pla@udg.es*

[b] *Dr. R. Eritja*
*Departament de Biologia Estructural*
*Institut de Biologia Molecular de Barcelona (IBMB)*
*Consejo superior de Investigaciones Científicas (CSIC)*
*Jordi Girona 18–26, 08034 Barcelona (Spain)*

[c] *Dr. M. Pla*
*Institut de Tecnologia Agroalimentària (INTEA)*
*Universitat de Girona, Campus Montilivi (Edif. Politècnica 1)*
*17071 Girona (Spain)*
*Fax: (+34) 972-418-399*

  DOI: 10.1002/cbic.200400358 

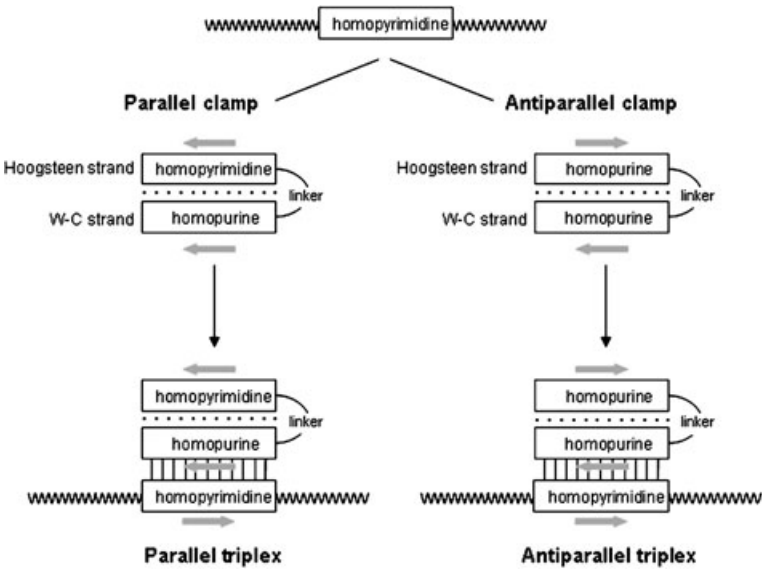


**Scheme 1.** Schematic representation of binding of a homopyrimidine single-stranded nucleic acid with parallel and antiparallel clamps. Arrows indicate 5′ to 3′ orientation. Lines indicate Watson–Crick hydrogen bonds, and dots Hoogsteen or reverse-Hoogsteen hydrogen bonds.

target oligonucleotide within its DNA or RNA sequence context. Single-stranded nucleic acid molecules tend to adopt secondary structures that have an effect on intermolecular interactions.[20–23] Therefore, secondary structures may pose a substantial problem to the ability of clamps to approach the target sequence, and this has never been addressed to date.

The presented results raise the problem of the influence of secondary structure on triplex formation by clamps. They show correlation between predicted stable target secondary structures and poorly efficient triplex formation and present the design of a new strategy based on the addition of a tail sequence to parallel-stranded, antiparallel-stranded and modified clamps to form triple helices with structured DNA or RNA molecules. Finally, they validate the new tail-clamp strategy to overcome structural interference, concomitantly greatly increasing the stability of triplex binding.

## Results

### The P35S clamp specifically binds the *35S* target oligonucleotide

We designed and synthesized a parallel-stranded clamp (P35S clamp, Table 1) targeting a 12-homopyrimidine sequence of the *CaMV35S* promoter in order to assess the capacity of such clamps to form triple helices in a real DNA context. The homopurine portion of the P35S clamp should be able to hybridise the target through Watson–Crick bonding, and the inverted homopyrimidine portion of the P35S clamp should form a triplex by Hoogsteen hydrogen bonding (Scheme 2). Initial binding experiments were performed with a 33-nt oligonucleotide (33pyr, Table 1), flanked by nucleotides 479 and 511 of the *CaMV35S* promoter at 5′ and 3′, respectively, including the 12-homopyrimidine target sequence. Radioactively labelled target was incubated with increasing amounts of P35S clamp under triplex-forming conditions. Triplex formation was observed in all reaction mixtures containing clamp (Figure 1 A). The percentage of binding gradually increased with the molar excess of clamp, approaching 100 % at 50-fold. Thermal stability analyses (Table 2) further confirmed the affinity observed by gel-shift. Such values for triplex formation are similar to those previously described for the parallel R22 clamp and WC-11mer[4] under the same conditions, indicating that different target sequences can be suitable for triplex formation through parallel-stranded clamps.

Further, we also studied the specificity of binding with a 33-nt oligonucleotide complementary to the target sequence (33pur, Table 1) but including a homopurine instead of the homopyrimidine track and therefore not expected to form triplexes with P35S clamp. Indeed, no shifted bands were detected up to a 100-fold excess of clamp (Figure 1 B). In addition, we used a 32-nt oligonucleotide (32pyr, Table 1) incorporating a different 12-nucleotide homopyrimidine track and obtained negative results (data not shown); this indicated that the *CaMV35S* promoter triplexes were formed in a sequence-specific manner. As was to be expected, nonhomologous clamps did not show detectable binding with 33pyr under the same conditions (data not shown).

**Table 1.** Sequences of homopyrimidine targets and parallel- and antiparallel-stranded clamps prepared in this study.

| Name | Sequence |
|---|---|
| 33pyr | 5′-CGTCTTCTTTTTCCACGATGCTCCTCGTGGGTG-3′ |
| 33pur | 5′-CACCCACGAGGAGCATCGTGGAAAAAGAAGACG-3′ |
| 50pyr | 5′-TGAAGACGTGGTTGGAACGTCTTCTTTTTCCAC-GATGCTCCTCGTGGGTG-3′ |
| 50pur | 5′-CACCCACGAGGAGCATCGTGGAAAAAGAAGACGTTCCAACCACGTCTT-CA-3′ |
| 32pyr | 5′-TGGAATAATTTATCTTCTTCTTCTATTTATGT-3′ |
| 15(−) | 5′-CCAACCACGTCTTCA-3′ |
| 22pyr | 5′-GGTTGGAACGTCTTCTTTTTCC-3′ |
| RNA 22pyr | 5′-GGUUGGAACGUCUUCUUUUUCC-3′ |
| P35S clamp | biotin-5′-GGAAAAAGAAGA-3′-$(eg)_6$-3′-TCTTCTTTTTCC-5′ |
| P35S-T clamp | biotin-3′TCTTCTTTTTCC-5′-$(eg)_6$-5′-GGAAAAAGAAGACGTTCCAACC-3′ |
| PN35S-T clamp | biotin-3′-TCTTCTTTTTCC-5′-$(eg)_6$-5′-GGNAANAGNAGACGTTCCAACC-3′ |
| A35S clamp | biotin-5′-AGAAGAAAAAGG-TTTT-GGAAAAAGAAGA-3′ |
| A35S-T clamp | biotin-5′-AGAAGAAAAAGG-TTTT-GGAAAAAGAAGACGTTCCAACC-3′ |
| WC35S-T clamp | 5′-AGTGGTACTATA-TTTT-GGAAAAAGAAGACGTTCCAACC-3′ |

N = 8-aminoadenine, $(eg)_6$ = hexa(ethylene glycol), biotin = biotin-CONH-$(CH_2)_6$-O-phosphate

  

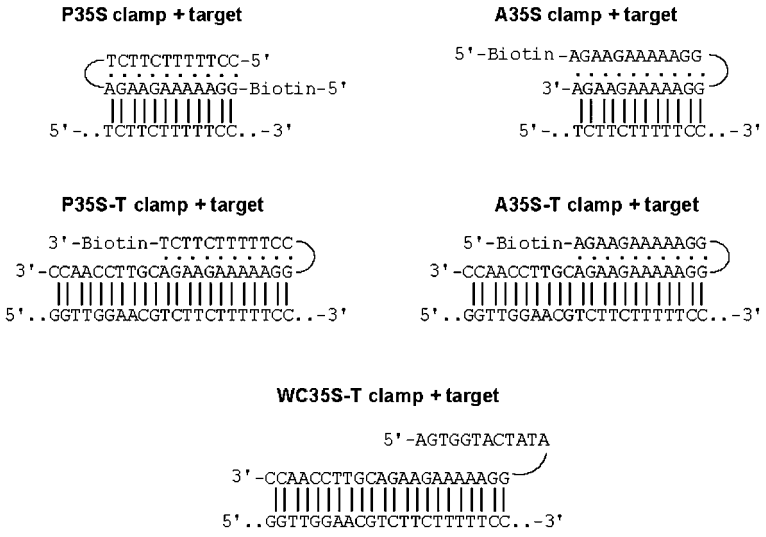


**Scheme 2.** Schematic representation of the theoretical interactions between 35S clamps and 35S tail-clamps and their target sequences.

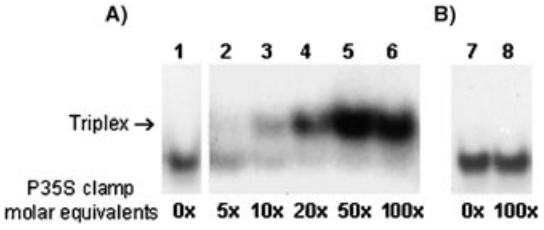


**Figure 1.** The P35S clamp specifically binds the *CaMV35S* promoter 33pyr oligonucleotide. A) Autoradiograph showing binding of P35S clamp to 33pyr oligonucleotide. Lanes 2–6: $^{32}$P-labelled target (2.5 nM) was incubated with 5–100 M equiv of cold clamp and the mixtures were analysed by 10% non-denaturing polyacrylamide gel electrophoresis at 4°C. Triplexes are indicated by the arrow. Lane 1: Control reaction without P35S clamp. B) Autoradiograph showing the lack of binding of P35S clamp to 33pur oligonucleotide (i.e., complementary to 33pyr). Lane 7: No clamp added to the reaction. Lane 8: Incubation of $^{32}$P-labelled 33pur with 100-fold P35S hairpin.

**Table 2.** Melting temperatures ($T_m$s) of triplexes in 0.1 M sodium phosphate and citric acid at the appropriate pH.

| Triplexes | pH | $T_m$ [°C][a] | $\Delta G$ [kcal mol$^{-1}$][a] |
|---|---|---|---|
| A35S clamp + 22pyr | 7.0 | 36.0 | −9.0 |
| A35S-T clamp + 22pyr | 7.0 | 62.7 | −18.7 |
| WC35S-T clamp + 22pyr | 7.0 | 58.4 | −14.1 |
| P35S clamp + 22pyr | 5.0 | 42.6 | −12.9 |
| P35S-T clamp + 22pyr | 5.0 | 55.1 | −14.8 |
| WC35S-T clamp + 22pyr | 5.0 | 51.1 | −12.1 |
| PN35S-T clamp + 22pyr | 5.0 | 56.2 | −16.0 |

[a] Uncertainties in $T_m$ values and free energies are estimated at ±1°C, and ±10%.

### Role of the secondary structure in triplex formation

Accessibility of the target sequence is a crucial requirement for successful interactions of nucleic acid molecules.[24,25] Single-stranded nucleic acid molecules tend to adopt secondary structures whose formation and stability can be theoretically predicted on a sequence basis by use of secondary structure prediction algorithms. Under our triplex-forming conditions, intramolecular target interactions could interfere with the intermolecular triplex formation. The 33pyr oligonucleotide used above was folded by use of the RNA Structure Version 4.11 program,[26] and no stable secondary structure involving the homopyrimidine track was predicted (Figure 2). However, it was predicted that a slightly longer sequence (50pyr, Table 1) should form a stable stem in which five out of 12 target pyrimidine nucleotides were involved in Watson–Crick intramolecular interactions (Figure 2). This stem was also predicted when longer (up to 600 nt) *CaMV35S* sequences were folded. Melting experiments with target (33pyr and 50pyr) oligonucleotides alone (at 2 μM concentration in 0.1 M sodium phosphate/citric acid pH 7.0) gave only a sigmoidal curve for oligonucleotide 50pyr. The melting temperature of the transition was 66°C ($\Delta G = -3.5$ kcal mol). This confirms the presence of a secondary structure in 50pyr under the experimental conditions.

Radioactively labelled 50pyr was incubated with increasing amounts of P35S clamp under triplex-forming conditions and analysed by gel-shift. Figure 3 shows the absence of lower mobility bands even at 100-fold excess of clamp, indicating the absence of triplexes. This could be due to inaccessibility of the target sequence as a result of the predicted intramolecular interactions (Figure 2). We therefore performed the same reactions in the presence of a 100-fold excess of 15(−) (Table 1), an oligonucleotide complementary to eight nucleotides in 50pyr involved in the same predicted intramolecular stem as the homopyrimidine track. Hybridization of 15(−) with 50pyr under standard triplex-forming conditions was confirmed (Figure 3). In the presence of 15(−), the P35S clamp was able to interact with 50pyr, although with low efficiency (Figure 3). This suggested that 15(−) should compete with the 50pyr predicted intramolecular stem and so make the homopyrimidine target sequence accessible. We concluded that such an intramolecular stem should contribute to the lack of triplex formation, and that such a problem could be overcome by competition of the intramolecular stem with a complementary oligonucleotide.

### Tail-clamps bind 35S target oligonucleotides with predicted secondary structures

One limitation of the use of two oligonucleotides to bind one target is the weak efficiency of trimolecular interactions. However, if the oligonucleotide is included as part of the clamp, it becomes possible to increase both the strength and the specificity of binding. We designed a new clamp molecule (a tail-clamp) by attaching an oligonucleotide (tail sequence, complementary to the 5′ flanking sequence of the homopyrimidine track) to its Watson–Crick-forming strand. The *CaMV35S* promoter tail-clamp (P35S-T clamp, Table 1) consists of: i) the same homopurine portion as the P35S clamp plus the adjacent tail

  

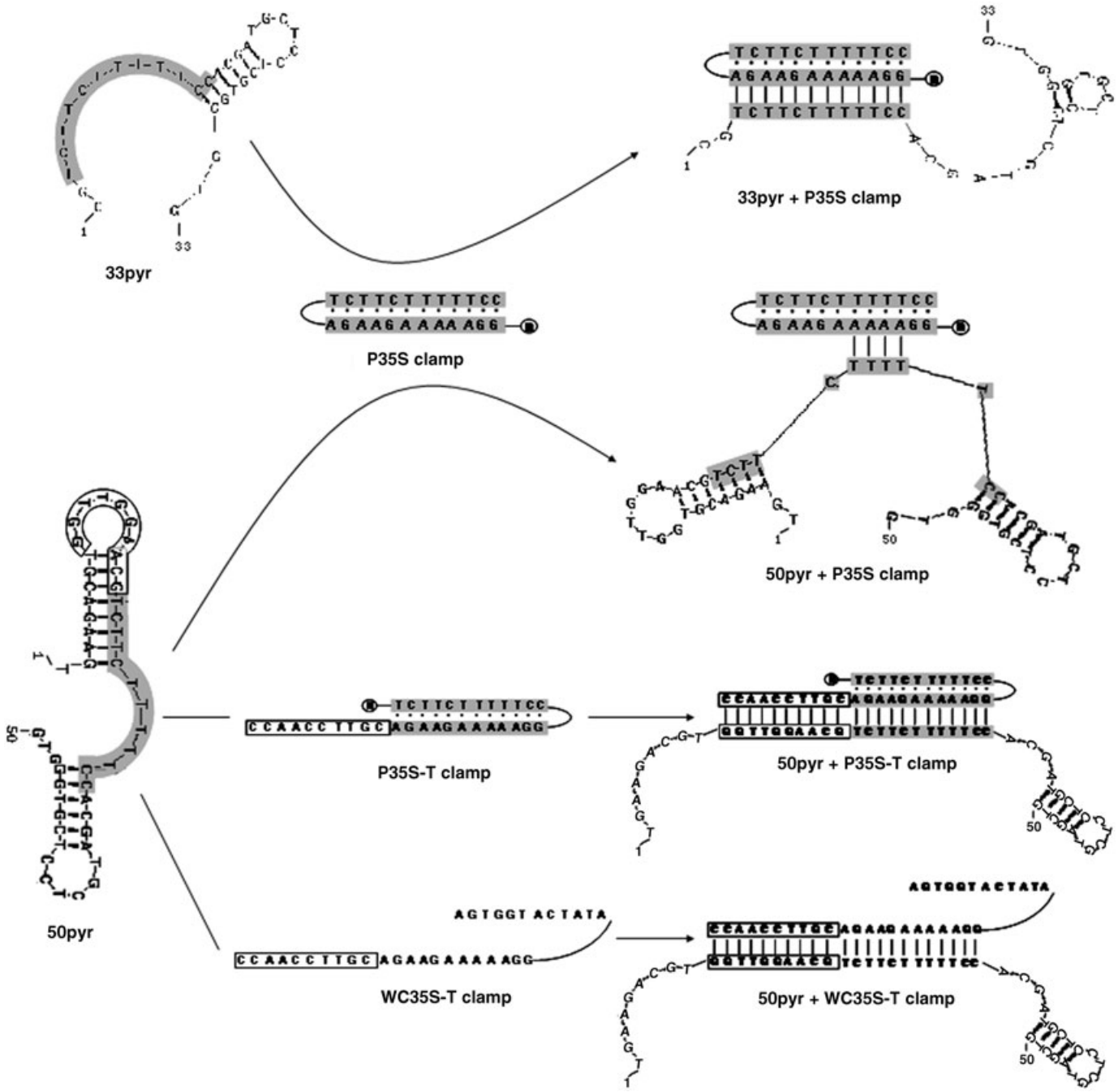


**Figure 2.** Predicted secondary structures in triplex formation. Diagram showing the predicted secondary structures of illustrative target oligonucleotides (33pyr and 50pyr) and clamps (35S clamps and 35S tail-clamps) used in this study, together with the anticipated bimolecular structures. Nucleotides intended to be involved in triplex formation are represented in grey boxes, while the tail sequence and its target are in white boxes. Lines indicate Watson–Crick hydrogen bonds, and dots Hoogsteen or reverse-Hoogsteen hydrogen bonds. The represented sequences correspond to parallel clamps or tail-clamps. The same bimolecular interactions are predicted for antiparallel clamps or tail-clamps.

sequence (Watson–Crick hydrogen bonds), and ii) the same inverted homopyrimidine portion as the P35S clamp (Hoogsteen hydrogen bonding) (Scheme 2). The tail element should assist the triplex formation by interfering with the tendency of the homopyrimidine target to form secondary structures with adjacent sequences (Figure 2).

Radioactively labelled 50pyr target was incubated with increasing amounts of P35S-T clamp under triplex-forming conditions and the results were analysed by gel-shift. In contrast to the negative results obtained with non-tailed clamps, binding with the tail-clamp was achieved, and it increased with the molar excess of P35S-T clamp up to around 45% at 100-fold (Figure 4A). Quantification of the shifted bands allowed calculation of the observed kinetic association constant ($k_{obs}$) (Table 3). The P35S-T clamp bound its target in a significantly more stable manner than the corresponding clamp in the ab-

  

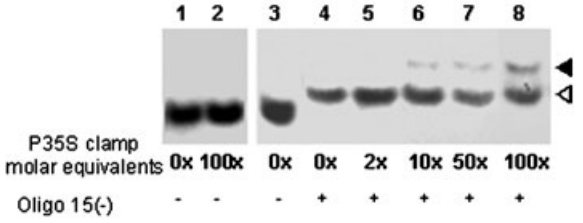


**Figure 3.** Role of secondary structure in triplex formation. Competition analysis showing binding of P35S clamp to $^{32}$P-labelled 50pyr in the presence of a 100-fold excess of oligonucleotide 15(−). Lane 2: Lack of binding of P35S clamp to $^{32}$P-labelled 50pyr in the absence of 15(−). Lanes 5–8: Binding reactions with 2–100 molar equivalents of cold clamp. The interaction of 50pyr and 15(−) is indicated by the open arrowhead. Interaction of 50pyr, 15(−) and P35S clamp is indicated by a solid arrowhead. Lane 4: Control reaction in the absence of P35S clamp. Lanes 1 and 3: 50pyr alone.

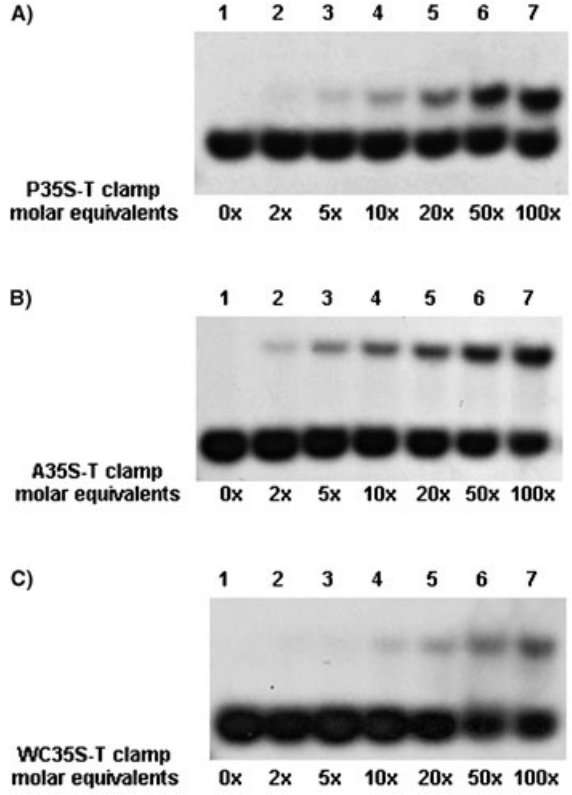


**Figure 4.** Tail-clamps efficiently bind structured 35S target oligonucleotides. Autoradiograph of 10% nondenaturing polyacrylamide gels run at 4°C showing binding of tail-clamps to 50pyr. Lanes 2–7: $^{32}$P-labelled target (2.5 nM) was incubated with 2–100 molar equivalents of cold tail-clamp. Lane 1: Control reaction in absence of tail-clamp. A) P35S-T clamp, shown under triplex-forming conditions (pH 5.0). B) A35S-T clamp (pH 7.0). C) WC35S-T clamp (pH 7.0).

sence of tail sequence, as shown by thermal stability analyses (difference in $T_m$: 12.5°C; difference in $\Delta G$: 1.9 kcal mol$^{-1}$; Table 2). In conclusion, tail-clamps are capable of overcoming structural impediments in triplex formation. The entropic effect obtained by linking two consecutive binding units results in a new molecule with higher affinity towards the target.

With the aim of obtaining triplexes that would be stable at neutral pH we studied the possible use of purine-rich clamps.

**Table 3.** Observed kinetic association constants ($k_{obs}$) for 50pyr and clamps used in this study.[a]

| Tail-clamp | pH | $k_{obs}$ [M$^{-1}$ s$^{-1}$] DNA[b] | RNA[b] |
|---|---|---|---|
| A35S clamp | 7.0 | n.d.[c] | |
| A35S-T clamp | 7.0 | 2500 | 4400 |
| WC35S-T clamp | 7.0 | 500 | |
| P35S clamp | 5.0 | n.d.[c] | |
| P35S-T clamp | 5.0 | 1400 | |
| WC35S-T clamp | 5.0 | 300 | |
| PN35S-T clamp | 5.0 | 2100 | 4800 |

[a] Calculated at a fivefold molar excess of clamp. [b] Uncertainties in $k_{obs}$ values are estimated at ±10%. [c] Binding not detected.

We thus designed and synthesized the A35S-T clamp (Table 1), an antiparallel tail-clamp that targets the same 12-homopyrimidine track of the *CaMV35S* promoter and incorporates the same tail sequence as the corresponding parallel tail-clamp. The A35S-T clamp should form triplexes with the target in the same manner as the P35-T clamp, except that the homopurine Hoogsteen strand should bind the double helical structure antiparallel to the target (Scheme 2). Binding of the A35S-T clamp was achieved with 50pyr up to around 55% at 100-fold excess (Figure 4B), as observed for the P35S-T clamp. Although not directly comparable (different pH conditions), it is interesting to note that both the $k_{obs}$ (Table 3) and the thermal stability (Table 2) values indicated a slightly higher stability for the complexes based on the antiparallel clamp than for those based on the corresponding parallel clamp.

We next evaluated the effect of the Hoogsteen bonds on the tail-clamp/target binding by using a control tail-clamp (WC35S-T clamp, Table 1) in which the Hoogsteen-forming strand was substituted by a random sequence and therefore could not form triplex. As would be expected, Watson–Crick interactions occurred (Figure 4C and Table 2 and Table 3), and these were weaker at pH 5.0 than at pH 7.0, possibly due to destabilisation of this type of interactions by protonation of cytosine and adenine residues at low pH. Interestingly, shifted bands resulting only from Watson–Crick interactions were significantly fainter (i.e., below 30% at 100-fold molar excess; Figure 4C) than those obtained with the A35S-T clamp and the P35S-T clamp. Affinity values obtained with the control, parallel or antiparallel tail-clamps and the *CaMV35S* target allowed the role of the Hoogsteen-forming strand to be quantified: triplex structures presented $k_{obs}$ values close to five times higher (Table 3), and thermal stability values showed important increments (difference in $T_m$: 4.0°C (parallel clamps) and 4.3°C (antiparallel clamps); difference in $\Delta G$: 2.7 and 4.6 kcal mol$^{-1}$, respectively). Therefore, Hoogsteen bonds contributed to the stabilization of structures involving the target and a parallel or antiparallel tail-clamp, which further confirmed that triplex structures were effectively formed.

In an attempt to increase the stability of triplex structures formed by parallel tail-clamps further, we synthesized and tested a modified P35S-T clamp with three 8-aminopurine nucleotides at the Watson–Crick-forming strand (PN35S-T clamp;

  

Table 1). Clamps incorporating 8-aminoadenine moieties have been shown to give very stable triple helical structures.[4] Under the same conditions, the PN35S-T clamp exhibited a stronger affinity than the unmodified clamp for the target [i.e., 1.5-fold higher $k_{obs}$ values (Table 3), difference in $T_m$ (1.1 °C) and difference in $\Delta G$ (1.2 kcal mol$^{-1}$; Table 2)]. As would be expected, no binding was observed if the control 50pur sequence was used as template, indicating triplex sequence specificity. Remarkably, the positive effect of 8-aminoadenine residues on the stability of triple helices previously observed in parallel clamps also proved to be valid for tail-clamps.

#### Tail-clamps efficiently bind RNA targets

Clamps have been shown to interact readily with complementary RNA single-stranded oligonucleotides, forming stable triplexes.[5] We next assessed the capacity of parallel and antiparallel tail-clamps to form triple helices with RNA targets. A radioactively labelled RNA22pyr (Table 1) target was incubated with increasing amounts of the PN35S-T clamp or the A35S-T clamp under triplex-forming conditions and analysed by gel-shift. The formation of triplex structures increased with the molar excess of clamps and approached 100% at 20-fold (data not shown). The $k_{obs}$ values (Table 3) indicated that parallel and antiparallel tail-clamps had superior affinities for RNA than for DNA targets. The sequence specificity was confirmed by use of nonhomologous RNA oligonucleotides and clamps (data not shown).

#### Triplex-mediated capture and recovery of *CaMV35S* target oligonucleotides

The increased stability of triple helices formed with tail-clamps and the potential to cope with structural impediments in the target sequences allow tail-clamps to be considered as an additional tool for analytical and therapeutic purposes. For instance, triplex formation has been used as one possible method for sequence-specific DNA purification (i.e., "triplex affinity capture",[27–32] based on the specific binding of a pyrimidine oligonucleotide to the purine strand in duplex DNA, forming a local triplex structure followed by capture of the triplex). In a prospective assay, we tested the suitability of tail-clamp-mediated triplex formation for the capture and recovery of RNA and DNA molecules with predicted secondary structures. As an example we used one of the tail-clamp molecules shown to form triple helices efficiently with structured targets (see above). We thus incubated radioactively labelled 50pyr or RNA22pyr target under triplex-forming conditions with a 50-fold excess of the biotinylated PN35S-T clamp previously bound to streptavidin-coated magnetic beads. Elution of the target was achieved by triplex destabilization and the process was monitored by denaturing acrylamide gel electrophoresis (Figure 5). Under the optimal conditions described in the Experimental Section, more than 50% (DNA target; Figure 5A) or 80% (RNA target, Figure 5B) of the initial radioactivity could be captured and recovered even in the presence of an excess of nontarget molecules (i.e., $10^3$-fold). No significant radioactivity (i.e., less than 3%) was found in the magnetic beads after elution. Moreover, less than 6% of the radioactivity was captured and recovered in parallel experiments in which the tail-clamp was either omitted or substituted by the corresponding nontailed clamp (P35S clamp). The $k_{obs}$, $T_m$ and $\Delta G$ values obtained with use of the PN35S-T clamp versus the WC35S-T clamp (Tables 2 and 3) indicated that although Watson–Crick interactions may have a role in our affinity capture assay; triplex formation should have a predominant role especially at pH 5.0. In conclusion, the method allowed efficient capture of target DNA or RNA and its subsequent recovery.

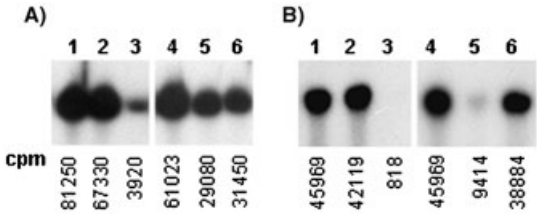


**Figure 5.** Triplex-mediated capture and recovery of *CaMV35S* promoter oligonucleotides by use of a biotin streptavidin recognition system. Autoradiograph of a 10% denaturing polyacrylamide gel showing capture of: A) $^{32}$P-labelled 50pyr, and B) $^{32}$P-labelled RNA 22pyr by triplex formation with PN35S-T clamp. Lanes 1–3: Control reactions in which the PN35S-T clamp was omitted. Lanes 1 and 4: Initial amount of oligonucleotide (250 fmol). Lanes 2 and 5: Uncaptured target. Lanes 3 and 6: Recovered (i.e., captured and eluted) target. Results of scintillation counting performed in a parallel experiment are indicated in counts per minute (cpm). Uncertainties in capture and recovery values are estimated at ±10%.

## Discussion

Targeting of suitable single strands through triplex formation by clamps has been proposed as a tool for molecular biological and gene expression studies. A flaw of these studies is that they have only been performed on homopyrimidine model target oligonucleotides. The major aim of this work is to assess the capacity of clamps to drive the formation of triple helices with homopyrimidine targets included within longer sequences and presenting predictable secondary structures. The formation of intramolecular structures has been reported to have an effect on intermolecular interactions involving nucleic acids such as small interfering RNAs,[20,33] antisense oligonucleotides[21,22] or *trans*-cleaving ribozymes.[23,34,35] Therefore, secondary structures may pose a substantial as yet unaddressed problem regarding the interaction of nucleic acid targets with clamps.

We selected a biologically relevant sequence—the *CaMV35S* promoter (a viral sequence commonly used for plant transformation)—containing a track of 12 pyrimidine nucleotides, five of them involved in a stable stem predicted by in silico folding and experimentally confirmed by thermal stability and competition analyses. The *CaMV35S* promoter-directed parallel clamp, which performed excellently with an oligonucleotide target of a size similar to previously reported short model oligonucleotides,[4] failed to bind the structured oligonucleotide 50pyr

  

over detectable levels. Therefore, the secondary structure of the homopyrimidine target and surrounding sequence has a significant and predictable effect on triplex formation (Figure 2).

New clamp molecules—that is, tail-clamps—were designed, and these efficiently formed triple helices in combination with structured target molecules (e.g., 50pyr). The tail sequence was incorporated in order to destabilize target intramolecular interactions and to allow the clamp portion of the tail-clamp to form the triplex efficiently (Figure 2). Tail sequences have been fused to other types of molecules with different purposes: to increase the strand invasion of double-stranded DNA by bis-PNAs,[36,37] for example, or, with catalytic RNAs, to increase the targeting efficiency of ribozyme M1 RNA (M1GS RNA ribozymes).[38,39]

We performed a comparative study on the interaction of the structured sequence 50pyr with tail-clamps, in which the clamp portion was either parallel- or antiparallel-stranded, and including 8-aminopurine nucleotide modifications when possible. By use of a combination of gel-shift, kinetic analysis, UV thermal melting and thermodynamic techniques, we demonstrated that all the tested tail-clamps efficiently bound the same structured target sequence, and that these interactions were indeed triplex structures. We had previously reported the formation of triplex structures by parallel, antiparallel and modified clamps with an unstructured model oligonucleotide.[4,15] Here we extend this finding to structured sequences with tail-clamps and establish that the tail-clamp tail portion does not inhibit the formation of triple helices but increases their stabilities. A series of experiments performed in parallel suggested that the orientation of the third strand with respect to the central homopurine Watson–Crick strand had consequences for the stability of triple helices. Antiparallel tail-clamps showed higher binding efficiencies than parallel tail-clamps (each under the optimal pH conditions). In addition, the reported triplex-stabilizing properties of 8-aminopurine residues[4] have been confirmed here for parallel tail-clamps (that is, the inclusion of three 8-aminopurine residues stabilized the triplex structures up to levels similar to those obtained with unmodified antiparallel tail-clamps). In accordance with previous results, the inclusion of a larger number of modified residues could enhance the binding efficiency. Unfortunately the high number of thymine residues in our target sequence and the fact that 8-aminoadenine destabilized antiparallel triplexes[15] did not allow the inclusion of modified residues in the antiparallel tail-clamp.

RNA molecules are typically found as single-stranded nucleic acids and mostly fold in stable secondary structures. RNA oligonucleotides had been reported to form stable triple structures with parallel-stranded conventional clamps, whether containing 8-aminoadenine residues[10] or not,[5] and with antiparallel clamps.[13,40] Here we have demonstrated that both antiparallel and modified parallel tail-clamps were able to bind an RNA target in a very efficient manner.

Tail-clamps can be regarded as an additional tool for nucleic acids studies. The specific properties of triple helices formed by parallel and antiparallel clamps may have important practical implications. Parallel clamps have been reported to form stable triplexes under acidic conditions, and these structures are relatively unstable at neutral and basic pH. They could be suitable for—for example—in vitro sequence enrichment purposes. In a prospective assay, we have shown the suitability of tail-clamps for specific capture and recovery of structured DNA and RNA targets by triplex affinity capture. In contrast, antiparallel triplexes are more promising in the biomedical field, since their stability is pH-independent, and they could be formed, for example, inside the cell.[41]

## Experimental Section

**Selection of a target sequence for triplex formation within the *CaMV35S* promoter**: A suitable homopyrimidine track for triplex formation in the *CaMV35S* promoter sequence was selected. It is 12 nucleotides long and located at positions 498 to 509 (according to Accession Number AR271019); that is, internal to the amplicon of the validated PCR assay and in a region conserved among most approved GMO events. Being of a similar length to the model sequence used to develop the clamp technology,[4] it should be capable of forming sequence-specific triplexes in combination with an appropriate clamp.

**Synthesis of unmodified oligonucleotides**: Oligonucleotides used in this study are listed in Table 1. Unmodified oligonucleotides [33pyr, 33pur, 50pyr, 50pur, 32pyr and 15(−)] were prepared and synthesized on an Applied Biosystems model 392 DNA synthesizer. Sequences were prepared with standard (Bz- or *i*Bu-protected) 3′-phosphoramidites and polystyrene solid supports (LV200) by the manufacturer's protocols. Coupling efficiencies were higher than 98%. After the assembly of the sequences, oligonucleotide supports were treated with aqueous ammonia (32%) at 55°C for 16 h. Ammonia solutions were concentrated to dryness and the products were desalted on NAP-10 (Sephadex G-25) columns eluted with water. The lengths and homogeneities of the products were checked by denaturing polyacrylamide gel electrophoresis. All the sequences were used without further purification. RNA oligonucleotides were purchased from Dharmacon.

**Single-stranded DNA folding and secondary structure prediction**: Single-stranded DNA structures were predicted with the aid of the RNAstructure program, Version 4.11.[26] Both 35S target oligonucleotides and a 600-nt sequence comprising the target sequence of the *CaMV35S* promoter were analysed.

**Synthesis of 35S clamps**: The parallel-stranded P35S clamp (Table 1) was designed with the purine sequence complementary to the *CaMV35S* promoter homopyrimidine target sequence, connected head-to-head and through their 3′-ends with the Hoogsteen C,T-sequence. A hexa(ethylene glycol) [$(eg)_6$] molecule was used to connect the two strands. A biotin molecule was added at one of the ends to allow capture by streptavidin.

Clamps P35S-T and PN35S-T (Table 1) have similar compositions, with the homopurine and the homopyrimidine parts connected through their 5′ ends with the hexa(ethylene glycol) linker [$(eg)_6$]. The P35S-T clamp has ten additional bases. These additional bases are complementary to the *CaMV35S* promoter after the homopyrimidine track, so the tail-clamp oligonucleotides should form a duplex after the triplex. A biotin molecule was also added at one of the ends. Finally, the PN35S-T clamp (Table 1) has the same sequence as the P35S-T clamp but three adenines are replaced by three 8-aminoadenines.

  

The oligonucleotides were prepared on an automatic Applied Biosystems 392 DNA synthesizer. The parallel clamps were prepared as described elsewhere.[4] The 5′–5′ clamps (P35S-T and PN35S-T) were prepared in four steps. Firstly, the pyrimidine part was prepared by use of reversed C and T phosphoramidites and reversed C-support (linked to the support through the 5′ end). Secondly, a hexa(ethylene glycol) linker was added by use of a commercially available phosphoramidite (Glen Research). Thirdly, the purine part was assembled from standard phosphoramidites for the natural bases and the 8-aminoadenine phosphoramidites. The phosphoramidite of 8-aminoadenine was prepared as described elsewhere.[4] Finally, biotin was added at the end of the sequence by use of a commercially available 5′-biotin phosphoramidite (Glen Research).

A similar approach was used for the preparation of the 3′–3′ clamp (P35S clamp). In this case, the purine part was assembled first, followed by the hexa(ethylene glycol). The pyrimidine part was the last to be assembled, by use of reversed phosphoramidites. After the assembly of the sequences, oligonucleotide supports were treated with aqueous ammonia (32%) at 55°C for 16 h. The ammonia solutions were concentrated to dryness and the products were purified by reversed-phase HPLC. Oligonucleotides were synthesized on a 200 nmol scale on polystyrene supports and with the last dimethoxytrityl (DMT) group at the 5′ end (DMT-on protocol) to facilitate reversed-phase purification. Each purified product presented a major peak, which was collected. Yields (OD units at 260 nm after HPLC purification) were between 5–10 OD. HPLC conditions: HPLC solutions were as follows. Solvent A: Acetonitrile (ACN; 5%) in triethylammonium acetate (pH 6.5, 100 mM) and solvent B: ACN (70%) in triethylammonium acetate (pH 6.5, 100 mM). Columns: PRP-1 (Hamilton), 250×10 mm. Flow rate: 3 mL min$^{-1}$. Linear gradients: 30 min 10–80% B (DMT-on) or 30 min 0–50% B (DMT-off).

The antiparallel clamp A35S (Table 1) was designed to have the purine sequence complementary to the *CaMV35S* promoter homopyrimidine target sequence, connected with the reverse Hoogsteen G,A-sequence. A tetrathymidine loop was used for connecting both strands, a biotin molecule being added at one of the ends to allow capture by streptavidin. The antiparallel tail-clamp A35S-T (Table 1) has ten additional bases as well as a biotin moiety at the 5′-end. Substitution of adenine with 8-aminoadenine is not possible in this context, as described in Ref. [15]. The control oligonucleotide sequence WC35S-T clamp has the complementary sequence to the *CaMV35S* promoter but a random sequence was added instead of the triplex-forming sequence. This oligonucleotide can only form a duplex with the target sequence. These oligonucleotides were synthesized and purified similarly to unmodified oligonucleotides as described above.

**Binding of clamps to target sequences by melting experiments**: Melting experiments were performed as follows. Solutions of equimolar amounts of clamps and the target strand (22pyr) were mixed in sodium phosphate/citric acid buffer (0.1 M) at the appropriate pH (parallel clamps pH 5.0 and antiparallel clamps pH 7.0). The DNA concentration was determined by UV absorbance measurements (260 nm) at 90°C, with use of the following extinction coefficients for the DNA coil state: 7500, 8500, 12500, 15000, and 15000 M$^{-1}$cm$^{-1}$ for C, T, G, A, and 8-amino-A, respectively. The solutions were heated to 90°C, allowed to cool slowly to room temperature, and stored at 4°C until the UV was measured. UV absorption spectra and melting experiments (absorbance vs. temperature) were recorded in 1 cm pathlength cells in a spectrophotometer, with a temperature controller and a programmed temperature increase rate of 0.5°C min$^{-1}$. Melts were run in duplicate at 260 nm and at a triplex concentration of 2 μM. All of the absorbance versus temperature plots showed sigmoidal curves indicating cooperative transitions, and the data were fitted to a two-state model by use of MeltWin 3.5 software[42] in order to determine the $T_m$ and $\Delta G$ values. Free energy values are given at 37°C. Uncertainties in $T_m$ values and free energies are estimated at ±1°C, and ±10%.

**Preparation of labelled targets**: The single-stranded *CaMV35S* target DNA or RNA oligonucleotides (100 pmol) were 5′-end-labelled with [$\gamma^{32}$P]ATP with T4 polynucleotide kinase in a final volume of kinase buffer (25 μl). After incubation at 37°C for 1 hour, the solution was heated at 70°C for 10 minutes to denature the enzyme and subsequently cooled to room temperature. The labelled oligonucleotide was precipitated in sodium acetate (pH 5.2, 0.3 M, 100 μL) containing glycogen (2 μg) with 2.5 volumes of cold ethanol. After overnight incubation at −20°C, the mixture was centrifuged at 4°C and 14000 r.p.m. for 45 min. The pellet was washed with ethanol (70%) and dissolved in water (100 μL).

**Conditions for triplex formation**: Radiolabelled targets (25 fmol) were heated at 93°C for 3 min in sodium phosphate/citric acid buffer [pH 5.0, 0.1 M (parallel clamps) or pH 7.0 (antiparallel clamps)], and cooled on ice for 1 min. Increasing amounts (two-, five-, ten-, 20-, 50- and 100-fold) of the 35S clamps were added, and the samples were incubated at 50/54°C in a final volume reaction (10 μl) for 1 h.

**Gel electrophoretic mobility shift analysis of the triplex formation**: Triplex formation reaction mixtures were treated with glycerol (60% *v/v*) and loaded onto nondenaturing polyacrylamide gels (10%) prepared with acrylamide/bisacrylamide 19:1 in sodium phosphate/citric acid buffer (pH 5.0 or pH 7.0, 0.1 M). Samples were run at 4°C and 60–70 V and results were visualized by autoradiography. The formation of triplex was monitored by the appearance of a radioactive band with lower mobility than that corresponding to the target alone. The gel was scanned on a phosphorimager (Molecular Dynamics), and shifted and unshifted bands were quantified with the aid of ImageQuant software (Molecular Dynamics). The observed kinetic association constants ($k_{obs}$) were estimated by calculation of the ratio of the shifted bands *vs*. total target (shifted plus unshifted bands) at a fivefold molar excess of clamp in a minimum of three independent experiments. Standard deviations were around 10% in all cases.

**Triplex affinity capture**: Streptavidin-coated magnetic beads (4 μL, Dynal Biotech) were thoroughly washed in buffer A [0.1 M sodium phosphate/citric acid buffer pH 5.0, NaCl (1 M)] before incubation with biotinylated clamps in a final volume (10 μL) of the same buffer for 30 min at room temperature. The beads were separated by use of a magnetic particle concentrator (Dynal Biotech) and were washed three times with sodium phosphate/citric acid buffer (pH 5.0, 0.1 M). They were subsequently used for triplex formation with radioactively labelled 50pyr or RNA22pyr target (250 fmol) as indicated. The beads were magnetically separated and the liquid phase was considered to contain uncaptured molecules. After three washes with sodium phosphate/citric acid buffer (pH 5.0, 0.1 M), the captured molecules were recovered by incubation in Tris buffer (pH 8, 0.1 M) for 10 min at 90°C, followed by magnetic separation of the beads. The process was monitored by denaturing polyacrylamide gel (10%) electrophoresis.

  

## Acknowledgements

*This work was supported by the Spanish Ministerio de Ciencia y Tecnología (grant INIA CAL01–058-C2–2) and the "La Marató de TV3" Foundation. We thank Prof. Pere Puigdomènech and Dr. Jordi Gómez for valuable suggestions. We also thank Dr. Anna Aviñó for synthesizing the P35S clamp.*

**Keywords:** antiparallel tail clamps · oligonucleotides · parallel tail clamps · RNA · structured targets

[1] N. T. Thuong, C. Hélène, *Angew. Chem.* **1993**, *105*, 697 – 723; *Angew. Chem. Int. Ed. Engl.* **1993**, *32*, 666 – 690.
[2] L. J. Maher III, *Bioessays* **1992**, *14*, 807 – 815.
[3] H. E. Moser, P. B. Dervan, *Science* **1987**, *238*, 645 – 650.
[4] A. Aviñó, M. Frieden, J. C. Morales, B. G. de la Torre, R. Güimil-García, F. Azorín, J. L. Gelpí, M. Orozco, C. González, R. Eritja, *Nucleic Acids Res.* **2002**, *30*, 2609 – 2619.
[5] E. R. Kandimalla, S. Agrawal, *Biochemistry* **1996**, *35*, 15 332 – 15 339.
[6] J. H. van de Sande, N. B. Ramsing, M. W. Germann, W. Elhorst, B. W. Kalisch, E. von Kitzing, R. T. Pon, R. C. Clegg, T. M. Jovin, *Science* **1988**, *241*, 551 – 557.
[7] A. Avino, J. C. Morales, M. Frieden, B. G. de la Torre, R. G. Garcia, E. Cubero, F. J. Luque, M. Orozco, F. Azorin, R. Eritja, *Bioorg. Med. Chem. Lett.* **2001**, *11*, 1761 – 1763.
[8] E. Cubero, A. Avino, B. G. de la Torre, M. Frieden, R. Eritja, F. J. Luque, C. Gonzalez, M. Orozco, *J. Am. Chem. Soc.* **2002**, *124*, 3133 – 3142.
[9] P. A. Beal, P. B. Dervan, *Science* **1991**, *251*, 1360 – 1363.
[10] A. Aviñó, M. G. Grimau, M. Frieden, R. Eritja, *Helv. Chim. Acta* **2004**, *87*, 303 – 316.
[11] E. T. Kool, *Chem. Rev.* **1997**, *97*, 1473 – 1488.
[12] M. Mills, P. B. Arimondo, L. Lacroix, T. Garestier, C. Hélène, H. Klump, J. L. Mergny, *J. Mol. Biol.* **1999**, *291*, 1035 – 1054.
[13] T. Vo, S. Wang, E. T. Kool, *Nucleic Acids Res.* **1995**, *23*, 2937 – 2944.
[14] J. Robles, A. Grandas, E. Pedroso, F. J. Luque, R. Eritja, M. Orozco, *Curr. Org. Chem.* **2002**, *6*, 1333 – 1368.
[15] A. Avino, E. Cubero, C. Gonzalez, R. Eritja, M. Orozco, *J. Am. Chem. Soc.* **2003**, *125*, 16 127 – 16 138.
[16] P. P. Chan, P. M. Glazer, *J. Mol. Med.* **1997**, *75*, 267 – 282.
[17] K. M. Vazquez, J. H. Wilson, *Trends Biochem. Sci.* **1998**, *23*, 4 – 9.
[18] C. Malvy, A. Harel-Bellan, L. L. Pritchard, *Triplex Helix Forming Oligonucleotides*, Kluwer, Dordrecht, **1999**.
[19] V. N. Soyfer, V. N. Potaman, *Triple Helical Nucleic Acids*, Springer, New York, **1996**.
[20] E. A. Bohula, A. J. Salisbury, M. Sohail, M. P. Playford, J. Riedemann, E. M. Southern, V. M. Macaulay, *J. Biol. Chem.* **2003**, *278*, 15 991 – 15 997.
[21] T. A. Vickers, J. R. Wyatt, S. M. Freier, *Nucleic Acids Res.* **2000**, *28*, 1340 – 1347.
[22] F. R. Kretschmer-Kazemi, G. Sczakiel, *Nucleic Acids Res.* **2003**, *31*, 4417 – 4424.
[23] T. B. Campbell, C. K. McDonald, M. Hagen, *Nucleic Acids Res.* **1997**, *25*, 4985 – 4993.
[24] A. D. Branch, *Trends Biochem. Sci.* **1998**, *23*, 45 – 50.
[25] M. Scherr, J. J. Rossi, G. Sczakiel, V. Patzel, *Nucleic Acids Res.* **2000**, *28*, 2455 – 2461.
[26] D. H. Mathews, M. D. Disney, J. L. Childs, S. J. Schroeder, M. Zuker, D. H. Turner, *Proc. Natl. Acad. Sci. USA* **2004**, *101*, 7287 – 7292.
[27] N. Bianchi, C. Rutigliano, M. Passadore, M. Tomassetti, L. Pippo, C. Mischiati, G. Feriotto, R. Gambari, *Biochem. J.* **1997**, *326*, 919 – 927.
[28] H. Ji, L. M. Smith, *Anal. Chem.* **1993**, *65*, 1323 – 1328.
[29] A. F. Johnson, R. Wang, H. Ji, D. Chen, R. A. Guilfoyle, L. M. Smith, *Anal. Biochem.* **1996**, *234*, 83 – 95.
[30] T. Kishida, M. Fukuda, K. Okazaki, W. Wang, Y. Tamaki, *Nippon Hoigaku Zasshi* **1996**, *50*, 255 – 257.
[31] S. V. Sonti, M. C. Griffor, T. Sano, S. Narayanswami, A. Bose, C. R. Cantor, A. P. Kausch, *Nucleic Acids Res.* **1995**, *23*, 3995 – 3996.
[32] T. Ito, C. L. Smith, C. R. Cantor, *Proc. Natl. Acad. Sci. USA* **1992**, *89*, 495 – 498.
[33] N. S. Lee, T. Dohjima, G. Bauer, H. Li, M. J. Li, A. Ehsani, P. Salvaterra, J. Rossi, *Nat. Biotechnol.* **2002**, *20*, 500 – 505.
[34] M. Amarzguioui, G. Brede, E. Babaie, M. Grotli, B. Sproat, H. Prydz, *Nucleic Acids Res.* **2000**, *28*, 4113 – 4124.
[35] A. Nadal, H. D. Robertson, J. Guardia, J. Gomez, *J. Gen. Virol.* **2003**, *84*, 1545 – 1548.
[36] T. Bentin, H. J. Larsen, P. E. Nielsen, *Biochemistry* **2003**, *42*, 13 987 – 13 995.
[37] K. Kaihatsu, R. H. Shah, X. Zhao, D. R. Corey, *Biochemistry* **2003**, *42*, 13 996 – 14 003.
[38] D. N. Frank, M. E. Harris, N. R. Pace, *Biochemistry* **1994**, *33*, 10 800 – 10 808.
[39] F. Liu, S. Altman, *Genes Dev.* **1995**, *9*, 471 – 480.
[40] S. Wang, E. T. Kool, *J. Am. Chem. Soc.* **1994**, *116*, 8857 – 8858.
[41] E. Washbrook, K. R. Fox, *Biochem. J.* **1994**, *301*, 569 – 575.
[42] J. A. McDowell, D. H. Turner, *Biochemistry* **1996**, *35*, 14 077 – 14 089.

Received: October 8, 2004
Published online on May 4, 2005

  